Egypt. J. Chem. **Vol. 68**, No. 5 pp. 431 - 443 (2025)

Egyptian Journal of Chemistry

http://ejchem.journals.ekb.eg/

Organic Geochemical Characteristics of Pre and Syn-Rift Source Rocks in the Geisum Concession, South Gulf of Suez, Egypt

Naira M. Lotfy [1]*, Sherif Farouk[1] , Ahmed k. ElBehery [2]

[1]*Exploration Department, Egyptian Petroleum Research Institute, Nasr City 11727, Egypt*

[2]*South Valley Egyptian Petroleum Holding Company- Nasser city - Cairo*

Abstract

This study provides a comprehensive geochemical analysis of pre-rift and syn-rift source rocks from the Geisum Concession, Gulf of Suez, utilizing biomarker distributions, Rock-Eval pyrolysis, and vitrinite reflectance data to evaluate hydrocarbon generation potential. Total Organic Carbon (TOC) values range from 1.0 to 7.27 wt%, with pre-rift formations showing higher organic content compared to syn-rift formations. The kerogen types identified span Type I, II, and III, with pre-rift formations predominantly containing Type II kerogen, suggesting a higher potential for oil generation. Biomarker analysis reveals a strong marine influence, evidenced by the dominance of C30 hopanes and the presence of C27 steranes, with minimal terrigenous input. The C32 homohopane ratios (22S/22R) indicate that the source rocks are in the early oil window, corroborated by Tmax, PI, and vitrinite reflectance (Ro%) data. Pre-rift formations show stratified, anoxic depositional conditions, while syn-rift formations exhibit less reducing environments. These findings suggest that pre-rift formations in deeper stratigraphic sections may offer higher hydrocarbon potential, particularly in the oil generation window. The results highlight the significance of these source rocks in regional petroleum exploration.

Keywords: Geisum Concession, Biomarkers, source rocks, thermal maturity

1. Introduction

The Gulf of Suez (GOS) is one of Egypt's Egypt's most productive regions for hydrocarbon extraction, with the Geisum Concession in the southern part of the basin playing a key role in its oil output (Fig.1). This area, situated within a tectonically active basin, has experienced multiple phases of rifting that shaped its structural and stratigraphic framework, creating favorable conditions for the generation, migration, and accumulation of hydrocarbons. The evaluation of the pre-rift and syn-rift source rocks in the Geisum Concession is essential to understanding the basin's petroleum system and its future hydrocarbon potential.

The pre-rift source rocks, which date from the Paleozoic to Oligocene, have had a longer geological history and have undergone deeper burial, making them more thermally mature compared to the younger syn-rift Miocene source rocks. However, organic-rich source rocks are present in both sequences, and the extent of their maturation is crucial for hydrocarbon generation. To assess the hydrocarbon generation potential of these source rocks, traditional geochemical analyses such as total organic carbon (TOC), Rock-Eval pyrolysis, and vitrinite reflectance provide foundational insights into their quality and maturity. In addition, biomarker characteristics like offer clues to the organic matter's origin, depositional environment, and degree of preservation. Several studies have examined the geological and geochemical attributes of source rocks in the Gulf of Suez, including the Geisum Concession [1–6]. The collective findings of these studies highlight the complex interplay between geological, tectonic, and geochemical factors that influence source rock potential in the Geisum Concession. The pre-rift source rocks, with their greater thermal maturity and longer geological history, are generally more favorable for hydrocarbon generation compared to the younger syn-rift formations. However, variations in burial depth, heat flow, and structural evolution create a heterogeneous landscape where some areas may have reached optimal maturation levels while others have not. Understanding the hydrocarbon potential of the Geisum Concession requires a detailed analysis of both pre-rift and syn-rift source rocks, this research is crucial for advancing the understanding of hydrocarbon systems in the Geisum Concession, guiding exploration and development efforts, and contributing to the sustainable management of the Gulf of Suez's valuable resources.

2. Stratigraphy and Geological setting

The Geisum Concession, situated in the South GOS, Egypt, is a geologically complex area with significant implications for hydrocarbon exploration (Fig.1). The region is underpinned by Precambrian basement rocks, which are primarily granites,

*Corresponding author e-mail: naira_epri@hotmail.com.; (Naira Magdy Lotfy).

Received date 11 September 2024; Revised date 23 September 2024; Accepted date 01 October 2024

DOI: 10.21608/ejchem.2024.320225.10411

gneisses, and schists. These crystalline rocks form the foundational base of the stratigraphic sequence and are crucial for understanding the geological history and structural framework of the area. Above the basement, the sedimentary sequence spans from the Mesozoic to the Cenozoic eras, reflecting a diverse range of depositional environments and tectonic influences. Three main tecctono-stratigraphic successions can be used to categorise the stratigraphy of the Gulf of Suez, which includes the Geisum Concession [10]. The lithostratigraphic units depicted in Fig. 2 provide more detail on this succession [5].

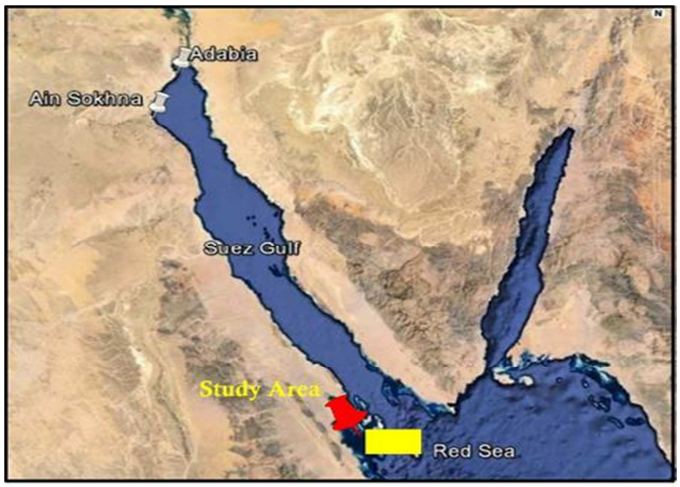

Figure 1: Location map of Geisum Concession

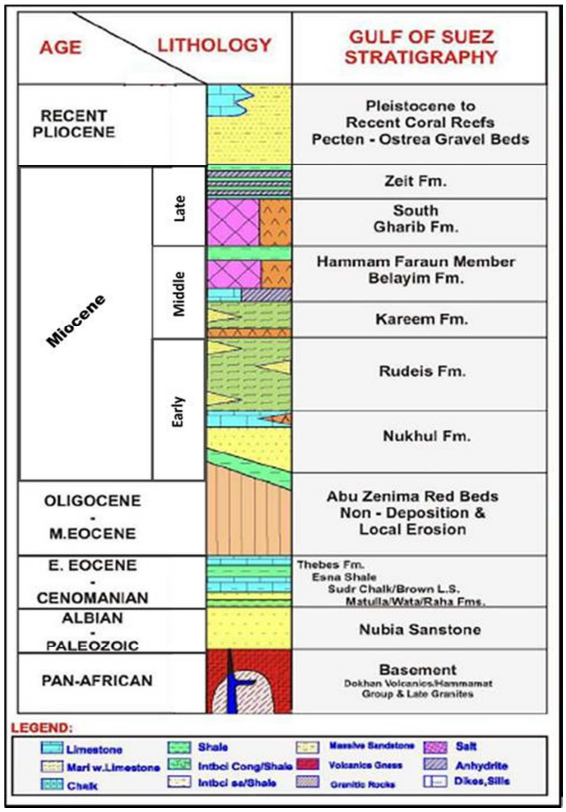

Figure 2: Stratigraphic column of South GOS showingthe studied formations

These consist of: (i) a pre-rift (pre-Miocene) succession from Paleozoic to Eocene; (ii) a synrift(syn Miocene) interval [11–13]; and (iii) a post-rift(post Miocene) interval [4,5]. The lithology andfacies of the described pre-rift and syn-rift successions, including the Nubian Complex,Cenomanian to Eocene formations, and the MioceneGharandal and Ras Malaab groups, are shown in detail in Fig. 2 [14,15]. The Gulf of Suez rift is a long, narrow graben formed by rifting that began in the Oligocene and continued into the post-Miocene period, extending as a northern continuation of the Red Sea – Gulf of Aden rift system. The Gulf of Suez features an asymmetric structure controlled by normal faults and tilted blocks, with changes in dip direction occurring twice along the rift. The Gulf of Suez rift is a long, narrow graben formed by rifting that began in the Oligocene and continued into the post-Miocene period, extending as a northern continuation of the Red Sea – Gulf of Aden rift system. The Gulf of Suez features an asymmetric structure controlled by normal faults and tilted blocks, with changes in dip direction occurring twice along the rift. Rifting significantly influenced the GoS's structural framework and the arrangement, thickness, and facies variations of the younger Paleogene deposits have been outlined. This tectonic activity influenced the distribution of oil, with NW–SE trending depressions serving as areas for the accumulation of thick, organic rich layers, while nearby fault-block highs functioned as oil reservoirs [4,5].

3. Research Materials and Procedures

Eighty-Four cutting samples were acquired from 7 exploration wells within the studied area, representing Pre-rift and Syn-rift formations. The organic content (TOC), kerogen nature, and thermal development (maturity) of the dispersed organic material in the analyzed rock samples were assessed using a Rock-Eval 6 Analyzer (RE6A), following the standard method described by [13] and based on the work of [14–16]. Eleven rock samples from various depths were chosen for biomarker analyses. The organic matter (soluble) were extracted from rock samples using a solvent (Chloroform,CHCl3) in a Soxhlet apparatus for 24 hours. Following this, asphaltenes were precipitated with n-hexane, and then the maltene were separated into aliphatic hydrocarbons, aromatic hydrocarbons, and polar fractions using alumina-silica gel column chromatography. The separation was achieved with n-hexane, benzene, and chloroform for the respective fractions. The saturate fraction of the extract were analyzed using gas chromatography (GC) and gas chromatography–mass spectrometry (GC–MS). Biomarker results (m/z 71 for n-alkanes, m/z 217 for steranes, m/z 191 for terpanes) were derived from peak intensity measurements. All of these analyses were conducted at the Stratochem Service Center.

4. Results and Discussion

4.1. Source rock features and their significance inoil and gas exploration

A great deal of study in the field of petroleum exploration, encompassing both traditional and non traditional techniques, highlights the importance of determining the properties of the source rock. These include the amount of organic matter, the type of kerogen, the potential for hydrocarbon formation, and thermal maturity, as noted by specialists like [20,21]. Table 1 presents a comparison of data from the pre and syn -rift formations, focusing on the correlation between TOC and Rock-Eval results. The total organic carbon (TOC) content of the analyzed rock units varies significantly, ranging from 1 to 7.27 weight percent (wt%). The Pre-rift formations, including the Wata, Matulla, Brown Limestone, Sudr, Thebes, and Esna formations, exhibit a broad spectrum of TOC values: 1.63–2.58 wt%, 1.45–3.70 wt%, 1.02–7.27 wt%, 1.39–7.09 wt%, and 1.25–3.37 wt%, respectively. In contrast, the Syn-rift formations, Nukhul and Rudeis, show lower TOC values, ranging from 1.08–1.59 wt% and 1.00–1.46 wt%, respectively. In terms of organic matter richness, previous studies have concluded that source rocks with TOC levels above 2 wt% are of excellent quality for hydrocarbon generation, as developed by [18].

In this study, the high TOC values observed in most Pre-rift formations, exceeding 1.5 weight percent (wt%)(Table 1), suggest outstanding source rock features with hydrocarbon generation potential rated from good to excellent. This assessment relies on the link between TOC levels and kerogen thermal degradation (S2). Meanwhile, the Syn-rift formations are classified as good source rocks (Table 1 & Fig. 3a). This result has been confirmed by[9,22]. Additionally, a few samples from the Syn-rift formations and most samples from the Pre-rift formations show higher free hydrocarbon values (S1) than TOC content. This reveals a weak positive correlation between TOC content and freehydrocarbon yield (S1), suggesting contamination by non-indigenous hydrocarbons [23] (Table 1& Fig.3b).

RE6A is a straightforward, cost-effective, and rapid assessment technique used to assess source rock capability, providing valuable insights into kerogen quality and thermal maturity. Organic matter quality and thermal evolution are typically assessed by graphing the hydrogen index (HI) against the T max, instead of using HI versus oxygen index (OI). As a result, kerogen-type classifications are based on HI to avoid reliance onoxygen index. Table 1 & Figure 4, which display HIand T max data, illustrate variations in kerogen types across different formations [24–29]. The samples from the Syn-rift formations (Nukhul and Rudeis) contain a mixture of type II/III kerogen. In contrast, the Pre-rift formations show a variety of kerogen types: the Wata and Matulla formations primarily contain type III kerogen, with only one sample exhibiting type II kerogen; the Brown Limestone, Sudr and Thebes formations are predominantly composed of type II and type I kerogen; and the Esna Formation contains both type II and mixed type II/III kerogen (Table 1&Fig.4)

Furthermore, the RE6A data (T max and PI) and vitrinite reflectance (Ro%) were used to assess the thermal maturity of the hydrocarbon generation capability of the analysed samples from the wells under study (Table 1).

Table (1): Results of organic carbon (TOC) and RE6A measurements

Well Name	Fm	Depth interval (Ft)	TOC wt %	S1(mg/g)	S2 mg/g	S3 mg/g	Tmax (ºC)	S2/TOC *100 (HI)	S3/ TOC *100(OI)	S1 /S1+S2(PI)	Measured Ro (%)	Calculated Ro (%)
GW-3	Rudeis	6160	1.18	0.46	3.12	1.28	423	264	108	0.13	0.37	0.45
		6200	1.16	0.95	3.94	1.56	422	340	134	0.19		0.44
		6270	1.03	0.7	2.91	1.71	423	283	166	0.19		0.45
Tawila W-2		10329	1.19	1.19	3.9	1.08	426	328	91	0.23		0.51
		10447	1.98	0.54	6.12	1.27	425	309	64	0.08	0.6	0.49
		10880	1.08	0.6	3.67	0.96	426	340	89	0.14	0.56	0.51
		11126	1.08	0.31	2.35	0.91	427	218	84	0.12	0.53	0.53
		11283	1.17	0.85	3.4	0.82	427	291	70	0.2	0.52	0.53
		11510	1.00	0.82	2.39	0.83	427	239	83	0.26		0.53
		11815	1.23	1.2	2.47	1.14	419	201	93	0.33		0.38
		11825	1.12	0.91	2.4	0.9	425	214	80	0.27		0.49
		11963	1.21	1.66	2.02	0.96	434	167	79	0.45	0.63	0.65
		12159	1.42	2.26	4.02	1.13	425	283	80	0.36	0.5	0.49
Tawila W-1		10391	1.08	0.82	2.86	1.19	428	265	110	0.22		0.54
		10450	1.46	0.98	5.19	1.25	423	355	86	0.16		0.45
Gw-3	Nukhul	6420	1.08	0.67	3.63	1.43	427	336	132	0.16		0.53
GW-2		9110	1.59	0.95	7.56	1.23	435	475	77	0.11		0.67
G-6	Thebes	5790	1.09	0.62	3.11	0.98	420	285	90	0.17		0.40
		5800	1.02	0.46	2.13	1.02	422	209	100	0.18		0.44
		5900	4.48	3.07	20.02	1.83	414	447	41	0.13		0.29
		5920	4.59	3.64	27.57	1.84	411	601	40	0.12		0.24
		5950	3.14	4.02	20.44	1.58	410	651	50	0.16		0.22
		5980	3.8	4.85	27.41	1.4	411	721	37	0.15		0.24
		6000	3.85	4.46	21.33	1.47	411	554	38	0.17		0.24
		6020	3.71	5.11	22.26	1.34	412	600	36	0.19		0.26
		6060	4.15	6.31	35.61	1.01	412	858	24	0.15	0.32	0.26
		6090	4.64	6.77	35.55	1.34	410	766	29	0.16		0.22
Tawila N-1		9571	1.23	0.16	5.95	0.51	418	484	41	0.03		0.36
GW-3	Esna	8560	1.25	1.61	6.04	1.16	435	483	93	0.21	0.54	0.67
GB-1		5080	1.25	0.23	3.82	1.57	428	306	126	0.06		0.54
		5180	2.64	0.35	9.04	1.75	424	342	66	0.04		0.47
		5240	1.72	0.33	4.72	1.77	419	274	103	0.07		0.38
G-13		4480	3.37	0.98	13.29	1.49	422	394	44	0.07		0.44
		4500	2.08	0.76	8.71	1.56	422	419	75	0.08		0.44
G-6	Sudr	6150	2.12	4.02	11.35	1.2	417	535	57	0.26		0.35
		6210	3.98	6.1	25.14	1.28	413	632	32	0.2		0.27
		6230	4.00	7.19	27.86	1.26	408	697	32	0.21		0.18
		6240	3.86	6.42	26.22	1.17	410	679	30	0.2		0.22
		6260	3.47	6.4	27.54	1.01	412	794	29	0.19		0.26
GB-1		5320	3.47	0.46	22.59	1.3	417	651	37	0.02		0.35
		5340	2.94	0.55	20.31	1.54	414	691	52	0.03		0.29
		5360	3.65	0.72	28.34	1.42	410	776	39	0.02		0.22
		5370	4.27	0.95	40	1.15	417	937	27	0.02		0.35

		5380	6.13	1.24	56.84	1.21	418	927	20	0.02		0.36
		5420	7.09	1	62.24	1.18	418	878	17	0.02		0.36
		5440	5.25	0.77	44.8	0.99	420	853	19	0.02		0.40
		5460	3.48	0.44	30.84	1	419	886	29	0.01		0.38
G-13		4520	1.39	0.74	4.16	1.65	419	299	119	0.15		0.38
		4540	1.99	0.75	6.1	1.77	417	307	89	0.11		0.35
		4560	1.83	1.24	7.11	1.71	417	389	93	0.15		0.35
		4570	2.02	1.26	7.17	1.71	418	355	85	0.15		0.36
		4590	2.83	1.11	11.52	1.78	415	407	63	0.09		0.31
		4610	2.95	1.32	14.9	1.61	412	505	55	0.08		0.26
		4630	2.77	0.97	14.18	1.71	414	512	62	0.06		0.29
		4650	2.84	1.16	16.77	1.58	413	590	56	0.06		0.27
		4670	3.6	1.15	22.62	1.41	413	628	39	0.05		0.27
		4680	3.52	2.27	27.95	1.37	414	794	39	0.08		0.29
G-6	Brown Limestone	6270	4.33	7.16	36.6	0.96	413	845	22	0.16		0.27
GB-1		5480	1.58	0.35	10.02	1.02	417	634	65	0.03		0.35
		5530	2.33	0.31	12.75	1.05	421	547	45	0.02		0.42
G-13		4720	6.91	4.62	73.54	1.43	414	1064	21	0.06	0.28	0.29
		4740	6.26	4.19	60.48	1.41	413	966	23	0.06		0.27
		4760	7.27	3.65	61.93	1.42	414	852	20	0.06		0.29
		4780	2.95	1.91	19.29	1.32	416	654	45	0.09		0.33
		4800	3.16	3.03	23.27	0.91	416	736	29	0.12		0.33
		4830	2.59	3	21.05	1.24	417	813	48	0.12		0.35
Tawila N-1		9886	2.37	0.31	14.97	1.18	423	632	50	0.02		0.45
		9895	2.48	0.31	19.48	1	422	785	40	0.02	0.31	0.44
		9915	1.99	0.23	14.2	0.84	421	714	42	0.02		0.42
		9925	1.02	0.11	4.66	0.6	424	457	59	0.02		0.47
GW-3	Matulla	9100	1.45	2.12	2.54	0.81	435	175	56	0.45	0.56	0.67
G-6		6800	2.58	2.23	5.09	1.29	427	197	50	0.3	0.48	0.53
GB-1		5690	2.01	0.75	2.65	2.73	421	132	136	0.22		0.42
		5730	1.52	0.34	1.71	2.1	420	113	138	0.17		0.40
		5790	1.67	0.35	1.44	1.88	411	86	113	0.2		0.24
G-13		4870	1.79	0.58	4.44	1.77	419	248	99	0.12	0.46	0.38
		4950	1.94	0.38	4.01	1.37	426	207	71	0.09		0.51
		4980	3.70	2.71	28.17	1.25	415	761	34	0.09		0.31
		5080	2.24	0.74	2.71	1.9	424	121	85	0.21		0.47
GB-1	Wata	5850	1.63	0.25	1.38	1.93	421	85	118	0.15		0.42
		5920	2.58	0.3	1.94	2.65	432	75	103	0.13		0.62

Notes

TOC, total organic carbon (wt%); S_2, hydrocarbons from kerogen cracking (mg HC/g rock); S_3, organic CO_2—kerogen derived (mg CO_2/g rock); T_{max}, pyrolysis temperature at which maximum emission of hydrocarbons occurs (°C); calculated $R_o = 0.0180 \times T_{max} - 7.16$; HI, hydrogen index = $S_2 \times 100/TOC$, OI, oxygen index = $S_3 \times 100/TOC$; PI, production index = $S_1/S_1 + S_2$

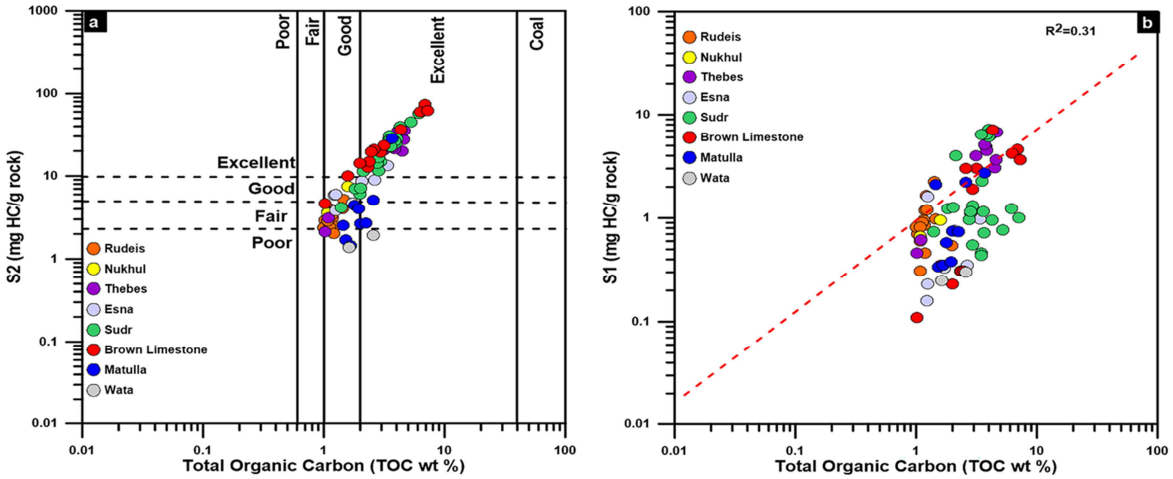

Figure 3: The cross-plot of TOC% against S1 and S2 (mg HC/g rock) illustrates the hydrocarbon generationpotential and indicates the presence of non-native hydrocarbons.

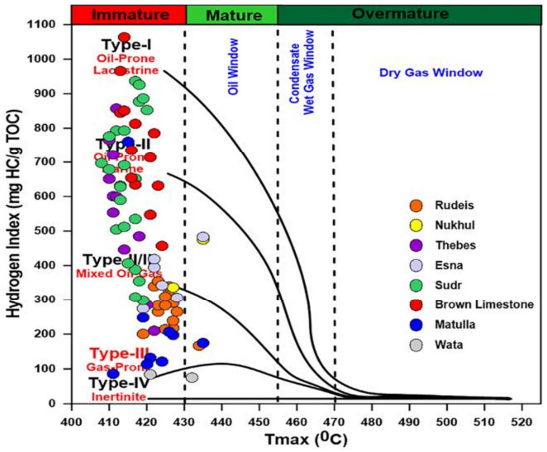

Figure 4: A plot of pyrolysis Tmax against the hydrogenindex (HI), revealing that the analyzed samples consisof various kerogen types and are primarily in thimmature to early oil window stages.

Vitrinite reflectance (Ro %) measurements are considered the most reliable for assessing organic maturation and the evolution of petroleum generation capacity [30]. In this study, all analyzed samples display low thermal maturity levels, with only a few samples indicating an early mature stage, as depicted in Figure 5. The thermal maturity levels determined by the Ro measurements are corroborated by the Tmax and PI readings

The thermal evolution of the selected samples was further evaluated using biomarker indicators [31–33] (Figs.6-7& Table 2). The C32 22S/(22S + 22R) ratio in C_{30} homohopanes, and the C29 regular and isomers sterane ratios ((20S/(20S + 20R) & ββ/(ββ + αα)) (Table 2), provided the most precise indicators of biomarker maturity. The occurrence of C_{32}-homohopane is used to determine the isomerization ratio of [22S/(22S + 22R)]. This ratio peaks at 0.70 with increasing thermal evolution (maturity). A ratio of C32 homohopanes less than 0.50 indicates immaturity in the source rock.

Source rocks in the early oil generation have ratios between 0.50 and 0.58; values greater than 0.58 suggest advanced maturation phases [32,34]. C32-homohopane ratios between 0.0.52 and 0.59 indicate that the samples under examination are in an early mature stage when viewed in the context of this scale (Table 2).

Furthermore, the C_{29} steranes, specifically 20S/(20S + 20R) and ββ/(ββ + αα), serve as indicators of the organic matter thermal evolution. According to [34,35], the main oil generation stage is typically achieved when the values exceed 0.30 and 0.40, respectively. The selected samples in this study exhibit ratios ranging from 0.27 to 0.40 for 20S/(20S + 20R) and from 0.37 to 0.41 for ββ/(ββ + αα), indicating a relatively low thermal maturity level for these formations (Table 2& Fig.8)

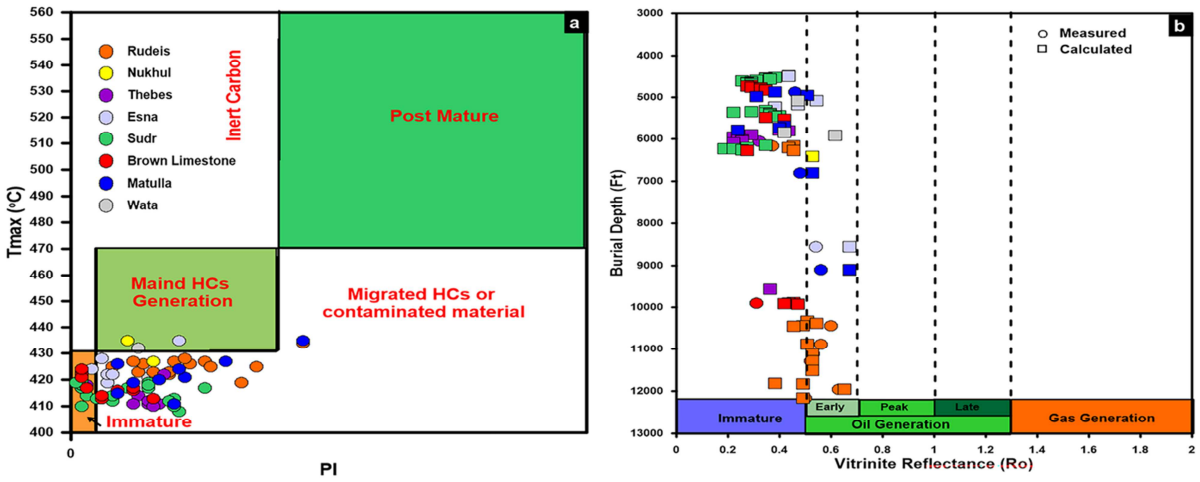

Figure 5: a) A plot of PI against Tmax,; b) Relationship between the measured, calculated Ro and burial depth in the studied wells, revealing that the analyzed samples are primarily in the immature to early oil window stages.

Table (2): Results of GC and GC/MS parameters of saturate fraction for cutting samples

Well Name	Fm	Depth (Ft)	GC (n-Alkanes and Isoprenoids)			Terpanes (m/z 191)										Steranes (m/z 217)			
			Pr/Ph	Pr/nC17	Ph/nC18	A	B	C	D	E	F	G	H	I	J	K	L	M	N
Tawila W-2	Rudeis	10447	1.34	0.97	0.85	0.08	2.18	0.7	0.73	0.02	0.35	0.20	0.62	0.59	37	30	33	0.32	0.37
GW-2	Nukhul	9110	1.39	0.71	0.59	0.22	1.95	0.9	0.9	0.04	1.08	0.40	0.65	0.59	28	30	42	0.33	0.40
G-13	Esnu	4480	0.99	0.59	0.78														
GA-2	Sudr	4040	0.79	0.5	0.72	0.04	2.47	1.23	0.6	0.99	0.32	0.34	1.54	0.52	35	33	32	0.27	0.41
G-9		4100	0.89	0.48	0.62														
GA-2	Brown Limestone	4330	0.78	0.58	0.81														
G-13		4740	0.55	0.47	0.87	0.07	2.87	1.36	0.9	0.34	0.44	0.41	1.39	0.53	32	40	29	0.3	0.37
G-9	Wata /Matulla	4820	0.84	0.49	0.63														
G-13		4980	0.55	0.47	0.87														
		4990	1.52	0.45	0.51														
G-11		5450	1.1	1.1	1	0.14	2.30	1	0.8	0.53	0.21	0.33	1.06	0.56	44	26	30	0.4	0.38

Notes: Pr/Ph: Pristane/Phytane ; A:C19/C23tricyclic terpanes ; B: C23/C24 tricyclic terpanes; C: C25/C26 tricyclic terpanes; D: C24 tetra/C26 tricyclic terpanes: E:Gammmacerane Index (GI) ; F: TS/Tm=C27 trisnorneohopane/trisnorhopane; G: C3122R homohopane/C30hopane;H: H35/H34 homohopanes; I: H32 S/S+R homohopanes ; J: %C27ααR steranes, K:% C28 ααR steranes L: %C29 ααR steranes M: C29αααS/S+R N:C29ββ(ββ+αα)

The biomarker maturity data are consistent with the maturity data previously obtained from VRo measurements and RE6A(Tmax &PI)(Figs 4-5&8). These findings indicate that the organic matter (primarily hydrogen-rich kerogen) within the studied formations in the studied wells has reached a low degree of maturity during the timeframe for oil generation. The Pre-rift and Syn-rift formations experienced varying burial depths and thermal gradients, with most formations entering the oil generation window during the Miocene. The thermal maturity ranges from immature to early mature, with deeper formations likely producing hydrocarbons, while shallower formations may have lower maturation levels (Fig.5b). At higher depths in Geisum concession, the Pre-rift and Syn-rift (Rudeis and Nukhul) likely reached significantly high levels of thermal maturity due to elevated burial temperatures. As a result, this deeper stratigraphic succession in the Geisum concession is considered a promising candidate for generating commercial quantities of oil and oil/gas in the region.

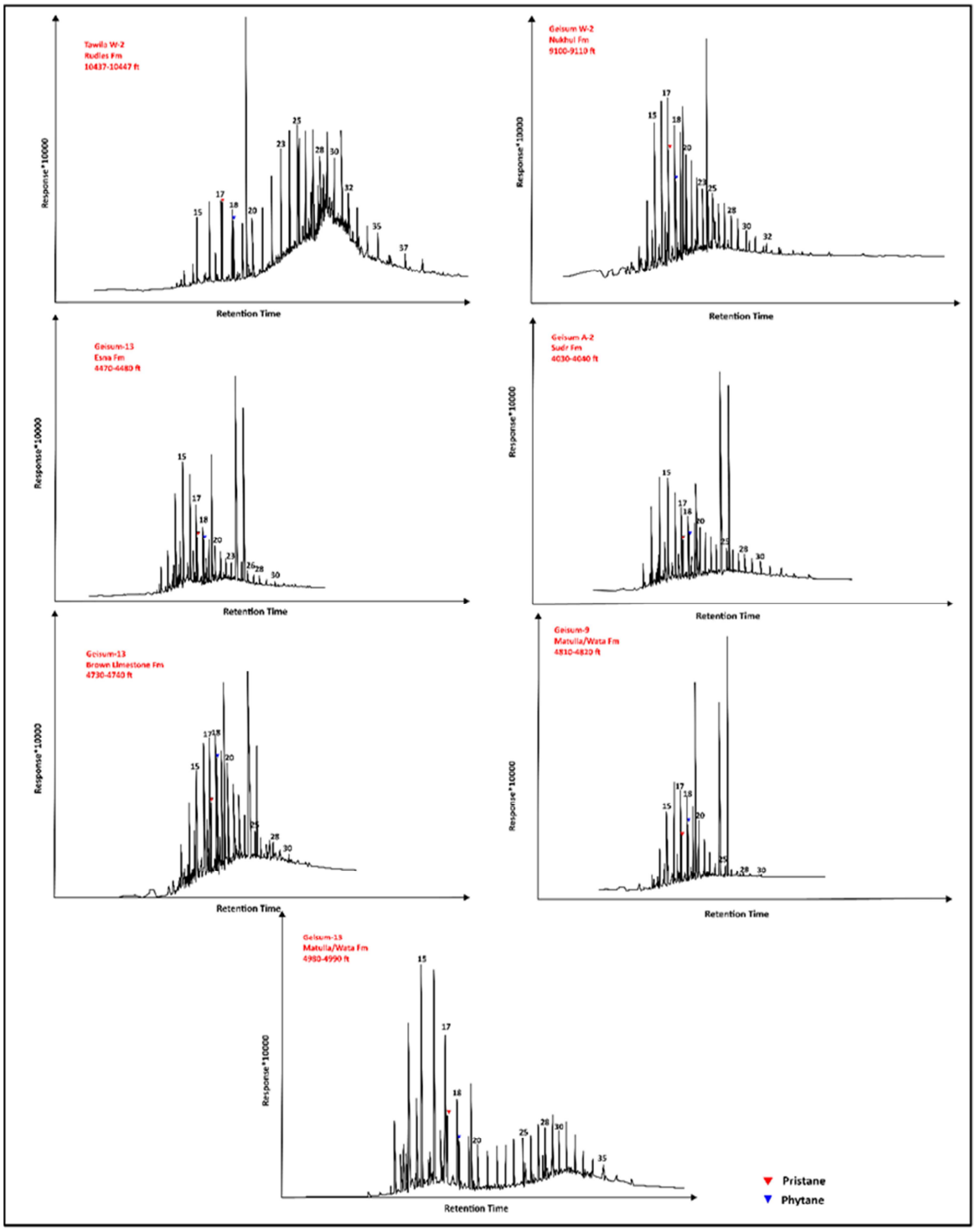

Figure 6: N-Alkanes and isoprenoids distribution of the aliphatic fraction.

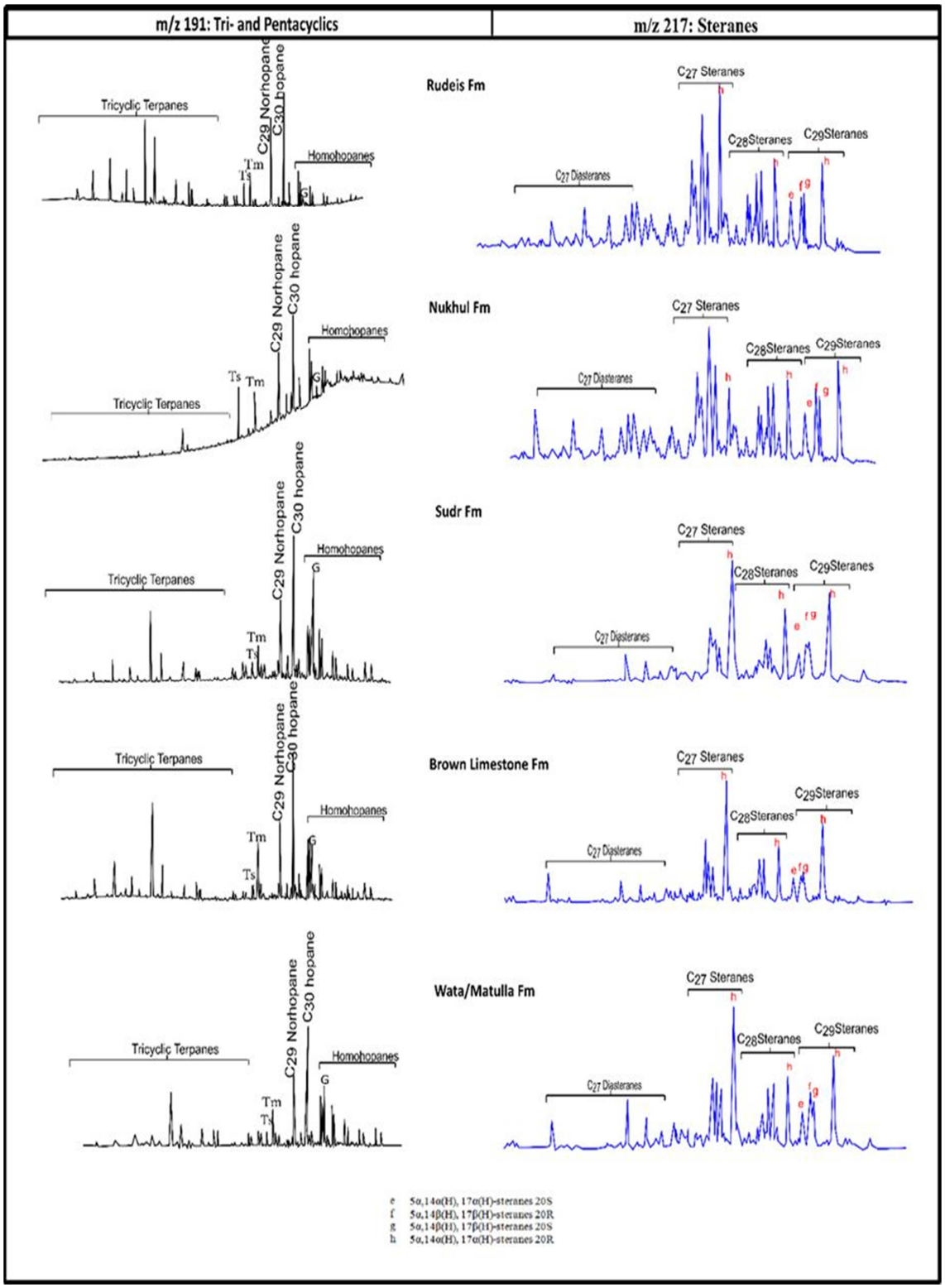

Figure 7: m/z 191 and 217 ion xhromatogram of the aliphatic fraction in rock samples.

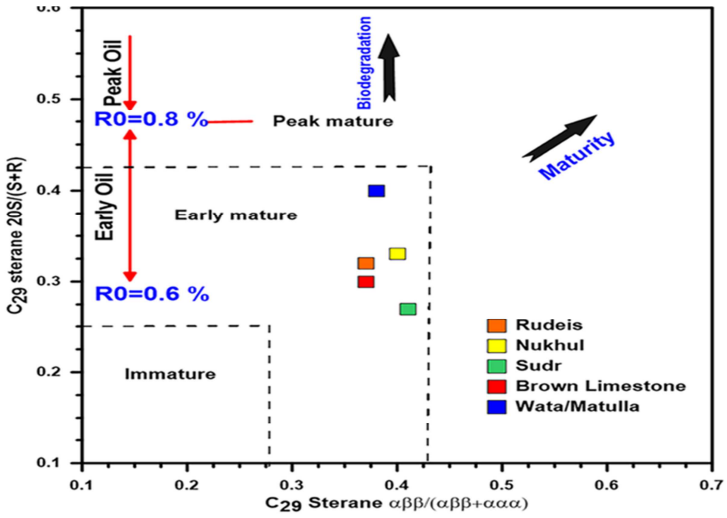

Figure 8: Cross-plot of the maturity-biomarker parameters (C29 sterane 20S/(20S + 20R) versus ßß/(ßß + aa) .

4.2. Organic matter contribution and sedimentary environmental characteristics

The organic matter (OM) contribution to the selected intervals, along with its origin and source, was evaluated using biomarker analysis. The distribution of biomarkers, along with their associated ratios and parameters, provided a basis for forming logical interpretations regarding the organic materialinput origin and the geological environmental conditions [36,37]. For sampled source rock extracts from the Geisum Concession, Figure 6 shows gas chromatograms of saturated hydrocarbons; Table 2 provides an overview of the data. Most extracts exhibit a unimodal n-alkane distribution skewed towards lower molecular weight compounds, with low concentrations of n-alkanesgreater than C23, and maxima typically between nC15 and nC20. However, the Rudeis extract and one sample from the Wata/Matulla extract show a bimodal n-alkane distribution. The Rudeis extract, in particular, displays significantly higher concentrations of nalkanes above C23 compared to the Nukhul and Wata/Matulla extracts. These characteristics, combined with the presence of acyclic isoprenoids (C19 pristane and C20 phytane), indicate deposition in carbonate environments under anoxic conditions, with significant contributions of algal or bacterial organic matter [38].

Phytane (Ph) levels are notably higher than pristane (Pr), with most samples exhibiting a Pr/Ph ratio of less than 1. This high phytane abundance and low Pr/Ph ratios point to the influence of halophilic bacteria and elevated sulfur content in the marine deposits[39]. However, some samples from the Wata/Matulla, Nukhul, and Rudeis formations have Pr/Ph ratios greater than 1.0, indicating a mixture of terrigenous and algal-derived organic matter deposited under highly reducing settings[40]. The isoprenoid/n-carbons ratios, represented by Pr/nC17 and Ph/nC18 (Table 2), are commonly applied to infer evidence about the origin, maturity, and decomposition levels of organic matter (biodegradation)[34]. In the investigated samples, pristane (Pr) and phytane (Ph) occur in moderate abundance relative to the n-alkanes (Table 2). The terrigenous input is negligible in three extract samples from the Wata/Matulla, Nukhul, and Rudeis formations. The organic material is largely categorized as oil-generating Type II and mixed Type II/III kerogens, predominantly deposited in an oxygen deficient environment with highly reducing conditions (Fig.9).

Biomarkers serve as essential geochemical indicators (Table 2; Fig. 7), provide detailed insights into the origin of organic matter [9,26,38]. Geisum source rocks, composed of shale, marl, and carbonates, contain mainly algal and bacterial organic matter with minimal higher plant input, reflected by low C19/C23, high C23/C24, and C25/C26 tricyclic terpane ratios, as well as relatively high C24 tetracyclic/C23 tricyclic terpane ratios [43,44](Table 2).

The widespread reducing environment is further supported by C35/C34 extended homohopane ratios exceeding 1, observed only in pre-rift extracts [45]. Additionally, gammacerane concentrations are notably higher in pre-rift formations compared to synrift formations. This suggests that the pre-rift sediments were placed in anoxic waters (saline to hypersaline) with a greater contribution from halophilic bacteria than the syn-rift extracts[38,45–47]. Moreover, the low Ts/Tm abundance in carbonate or shale/marl source rocks except for one sample from the Nukhul Formation where the Ts/Tm ratio is approximately 1 (Table 2), indicates either low thermal maturity or low clay concentration[34,38].

As noticed in figure 6 and table 2, The C30 hopane is predominant over the C31R homohopane, exhibiting moderate to high values, ranging from 0.20 to 0.40 in the syn-rift formations and 0.33 to 0.41 in the pre-rift formations (Table 2). These values suggesta marine depositional environment, as values exceeding 0.25 typically indicate marine settings [34,38]. This interpretation is further supported by the relationship between the C31R/C30 hopane and Pr/Ph ratios (Fig.10a).

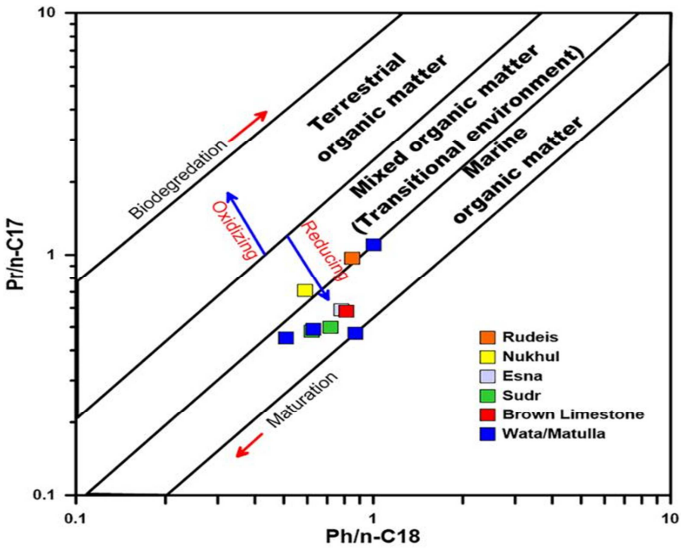

Figure 9: The plot of pristane/n-C17 versus phytane/n-C18 for the analyzed samples indicates that they predominantly originate from a marine depositional environment.

The sterane ternary plot (Fig. 10b) illustrates that most of the extract samples cluster within the region indicative of planktonic and bacterial organic matter [23]. In these samples, the dominance of C27 steranes, often occurring in comparable amounts to C29, indicates a predominance of marine organic matter (algae and bacteria)) with minimal landplant contributions, placed in anoxic reducing settings [43].

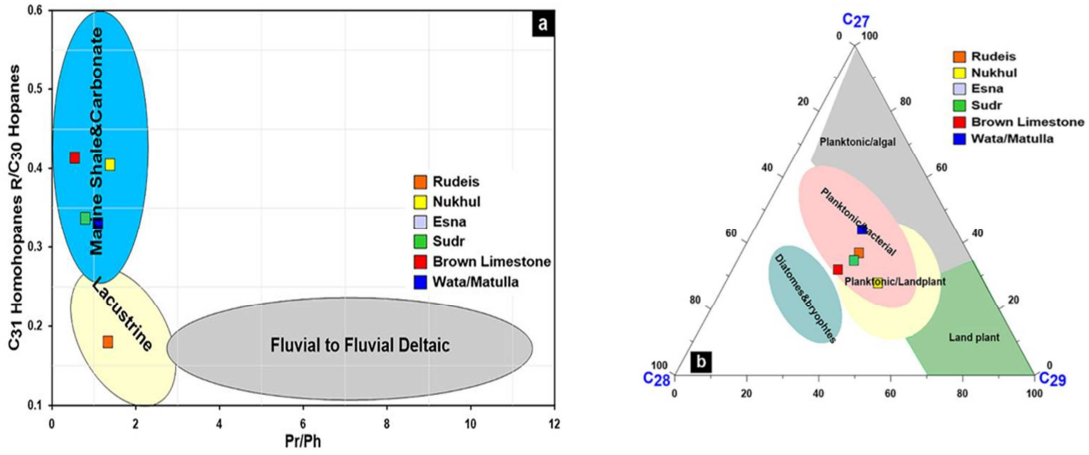

Figure 10: a) A plot of Pr/Ph versus C31homohopane/C30 hopane, b)Regular steranes (C27-C29) ternary plot, showing the depositional environment facies and origin of organic matter input.

5. Conclusion

The geochemical and maturity analysis of source rocks from the Geisum Concession demonstrates a clear distinction between pre-rift and syn-riftformations in terms of organic richness, kerogen type, and depositional environment. Pre-rift formations, with higher TOC values and Type II kerogen, show significant oil generation potential, especially in deeper stratigraphic layers where thermal maturity is greater. Syn-rift formations, while exhibiting lower TOC and mixed Type II/III kerogen, still display favorable characteristics for hydrocarbon generation, albeit to a lesser extent.

Biomarker data indicate a strong marine organic matter input for both pre- and syn-rift formations, with C_{30} hopanes and C_{27} steranes dominating the extracts, pointing to deposition in anoxic to mildly reducing environments. The elevated C_{32} homohopane ratios in pre-rift formations confirm early oil generation maturity levels, supported by Tmax, PI, and vitrinite reflectance results. The occurrence of gammacerane in higher concentrations in pre-rift formations furthersuggests deposition in hypersaline, stratified waters, likely with significant bacterial contributions. Overall, the study highlights that pre-rift formations, particularly at greater depths, hold considerable potential for hydrocarbon generation, making them promising targets for further petroleum exploration in the Gulf of Suez region.

6. Conflicts of interest

"There are no conflicts to declare"

7. Acknowledgments

The data used in this study was provided by the Egyptian General Petroleum Corporation (EGPC), for which the authors are thankful. Additionally, the author is grateful to the Egyptian Petroleum Research Institute (EPRI) for providing laboratory facilities and supporting the analysis.

8. References

[1]M.K. El Ayouty, in: Petroleum Geology., In: R. Said (Ed.),The Geology of Egypt, Rotterdam, Balkema, 1990: pp. 567-599.

[2]W.Sh. El Diasty, K.E. Peters, Genetic classification of oil families in the central and southern sectors of the Gulf of Suez, Egypt, Journal of Petroleum Geology 37 (2014) 105–126. https://doi.org/10.1111/jpg.12573.

[3]K.I. Schütz, Structure and Stratigraphy of the Gulf of Suez, Egypt, in: Interior Rift Basins, American Association of Petroleum Geologists, 1994. https://doi.org/10.1306/M59582C3.

[4]M. Darwish, A.-M. El-Araby, Petrography and diagenetic aspects of some siliclastic hydrocarbon reservoir in relation to the rifting of the Gulf of Suez, Egypt, Geol. Soc. Egypt Spec. Publ. No.1 (1993) 155–187.

[5]A.S. Alsharhan, Petroleum geology and potential hydrocarbon plays in the Gulf of Suez rift basin, Egypt, AAPG Bulletin 87 (2003) 143–180. https://doi.org/10.1306/062002870143.

[6]W. Bosworth, S. Durocher, Present-day stress fields of the Gulf of Suez (Egypt) based on exploratory well data: Non-uniform regional extension and its relation to inherited structures and local plate motion, Journal of African Earth Sciences 136 (2017) 136–147. https://doi.org/10.1016/j.jafrearsci.2017.04.025.

[7]M.M. El Nady, F.S. Ramadan, M.M. Hammad, N.M. Lotfy, Evaluation of organic matters, hydrocarbon potential and thermal maturity of source rocks based on geochemical and statistical methods: Case study of source rocks in Ras Gharib oilfield, central Gulf of Suez, Egypt, Egyptian Journal of Petroleum 24 (2015) 203–211. https://doi.org/10.1016/j.ejpe.2015.05.012.

[8]M.M. El-Nady, N.M. Lotfy, Multivariate geochemical and statistical methods applied to assessment of organic matter potentiality and its correlation with hydrocarbon maturity parameters (Case study: Safir-1x well, North Western Desert, Egypt), Egyptian Journal of Petroleum 25 (2016) 555–563. https://doi.org/10.1016/j.ejpe.2015.12.001.

[9]W.Sh. El Diasty, S.Y. El Beialy, A.R. Mostafa, A.A. Abo Ghonaim, K.E. Peters, Chemometric Differentiation of Oil Families and Their Potential Source Rocks in the Gulf of Suez, Nat Resour Res 29 (2020) 2063–2102. https://doi.org/10.1007/s11053-019-09569-3.

[10] J.-C. Plaziat, C. Montenat, P. Barrier, M.-C. Janin, F. Orszag-Sperber, E. Philobbos, Stratigraphy of the Egyptian syn-rift deposits: correlations between axial and peripheral sequences of the north-western Red Sea and Gulf of Suez and their relations with tectonics and eustacy, in: B.H. Purser, D.W.J. Bosence (Eds.), Sedimentation and Tectonics in Rift Basins Red Sea:- Gulf of Aden, Springer Netherlands, Dordrecht, 1998: pp. 211–222. https://doi.org/10.1007/978-94-011-4930-3_13.

[11] S. El Beialy, M. Mahmoud, A. Ali, Insights on the age, climate and depositional environments of the Rudeis and Kareem formations, GS 78-1 Well, Gulf of Suez, Egypt: a palynological approach, Revista Española de Micropaleontolog'ia 37 (2005) 273–289.

[12] M.I. Al-Husseini, Late Oligocene–Early Miocene Nukhul Sequence, Gulf of Suez and Red Sea, GeoArabia 17 (2012) 17–44. https://doi.org/10.2113/geoarabia170117.

[13] H. El Atfy, R. Brocke, D. Uhl, Age and paleoenvironment of the Nukhul Formation, Gulf of Suez, Egypt: Insights from palynology, palynofacies and organic geochemistry, GeoArabia 18 (2013) 137–174. https://doi.org/10.2113/geoarabia1804137.

[14] W. Bosworth, S. Khalil, A. Clare, J. Comisky, H. Abdelal, T. Reed, G. Kokkoros, Integration of outcrop and subsurface data during the development of a naturally fractured Eocene carbonate reservoir at the East Ras Budran concession, Gulf of Suez, Egypt, SP 374 (2014) 333–360. https://doi.org/10.1144/SP374.3.

[15] M. Sarhan, M. Wady, E. Assal, M. Raia, Oil potentialities of West Esh El-Mallaha area, southern Gulf of Suez as deduced from well log data interpretation, Scientific Journal for Damietta Faculty of Science 13 (2023) 76–83. https://doi.org/10.21608/sjdfs.2023.224186.1122.

[16] F. Behar, V. Beaumont, H.L. De B. Penteado, Rock-Eval 6 Technology: Performances and Developments, Oil & Gas Science and Technology - Rev. IFP 56 (2001) 111–134. https://doi.org/10.2516/ogst:2001013.

[17] J. Espitalié, J.L. Laporte, M. Madec, F. Marquis, P. Leplat, J. Paulet, A. Boutefeu, Méthode rapide de caractérisation des roches mètres, de leur potentiel pétrolier et de leur degré d'évolution, Rev. Inst. Fr. Pét. 32 (1977) 23–42. https://doi.org/10.2516/ogst:1977002.

[18] K.E. Peters, Guidelines for Evaluating Petroleum Source Rock Using Programmed Pyrolysis, AAPG Bulletin 70 (1986) 318-329. https://doi.org/10.1306/94885688-1704-11D7-8645000102C1865D.

[19] K. Peters, M. Cassa, Applied Source-Rock Geochemistry. In: Magoon, L.B. and Dow, W.G., Eds., The Petroleum System. From Source to Trap, AAPG Memoir, 1994.

[20] D.M. Jarvie, Shale Resource Systems for Oil and GasPart 2□Shale-oil Resource Systems, in: Shale Reservoirs—Giant Resources for the 21st Century, American Association of Petroleum Geologists, 2012. https://doi.org/10.1306/13321447M973489.

[21] P.C. Hackley, R.T. Ryder, Organic geochemistry and petrology of Devonian shale in eastern Ohio: Implications for petroleum systems assessment, Bulletin 105 (2021) 543–573. https://doi.org/10.1306/08192019076.
[22] W.Sh.E. Diasty, S.Y. El Beialy, R.M. El Attar, A. Khairy, K.E. Peters, D.J. Batten, Oil-source correlation in the West Esh El Mellaha, southwestern margin of the Gulf of Suez rift, Egypt, Journal of Petroleum Science and Engineering 180 (2019) 844–860. https://doi.org/10.1016/j.petrol.2019.05.083.
[23] J. Hunt, Petroleum Geochemistry and Geology, W.H. Freeman, New York, 1996.
[24] J. Espitalié, G. Deroo, F. Marquis, La pyrolyse Rock-Eval et ses applications. Deuxième partie., Revue de l'Institut Français Du Pétrole 40 (1985) 755–784.
[25] P.K. Mukhopadhyay, J.A. Wade, M.A. Kruge, Organic facies and maturation of Jurassic/Cretaceous rocks, and possible oil-source rock correlation based on pyrolysis of asphaltenes, Scotian Basin, Canada, Organic Geochemistry 22 (1995) 85–104. https://doi.org/10.1016/0146-6380(95)90010-1.
[26] B.P. Tissot, D.H. Welte, Petroleum Formation and Occurrence, Springer Berlin Heidelberg, Berlin,Heidelberg,1984. https://doi.org/10.1007/978-3-642-87813-8.
[27] J. Espitalié, G. Deroo, F. Marquis, La pyrolyse Rock-Eval et ses applications. Deuxième partie., Revue de l'Institut Français Du Pétrole 40 (1985) 755–784.
[28] E. Lafargue, F. Marquis, D. Pillot, Rock-Eval 6 Applications in Hydrocarbon Exploration, Production, and Soil Contamination Studies, Rev. Inst. Fr. Pét. 53 (1998) 421–437. https://doi.org/10.2516/ogst:1998036.
[29] H. Dembicki, Three common source rock evaluation errors made by geologists during prospect or play appraisals, Bulletin 93 (2009) 341–356. https://doi.org/10.1306/10230808076.
[30] Sweeney Jerry, A. Burnham, Evaluation of a simple model of vitrinite reflectance based on Chemical kinetics, Aapg Bulletin - AAPG BULL 74 (1990) 1559–1570.
[31] A.S. Mackenzie, R.L. Patience, J.R. Maxwell, M. Vandenbroucke, B. Durand, Molecular parameters of maturation in the Toarcian shales, Paris Basin, France—I. Changes in the configurations of acyclic isoprenoid alkanes, steranes and triterpanes, Geochimica et Cosmochimica Acta 44 (1980) 1709–1721. https://doi.org/10.1016/0016-7037(80)90222-7.
[32] W.K. Seifert, J.M. Moldowan, Use of biological markers in petroleum exploration, Methods in Geochemistry and Geophysics 24 (1986) 261–290.
[33] K.E. Peters, J.M. Moldowan, The biomarker guide: interpreting molecular fossils in petroleum and ancient sediments, Prentice Hall, Englewood Cliffs, N.J, 1993.
[34] K.E. Peters, J.M. Moldowan, The biomarker guide: interpreting molecular fossils in petroleum and ancient sediments, Prentice Hall, Englewood Cliffs, N.J, 1993.
[35] M.H. Hakimi, A. Kahal, A. Rahim, W. Naseem, W. Alsomid, A. Al-Buraihi, T. Alyousofi, S. Alqahtani, H.A. Alyousofi, N.M. Lotfy, Implications of Organic Matter Input, Sedimentary Environmental Conditions, and Gas Generation Potential of the Organic-Rich Shale in the Onshore Jiza-Qamar Basin, Yemen, ACS Omega 8 (2023) 30483–30499. https://doi.org/10.1021/acsomega.3c03691.
[36] D. Waples, T. Machihara, Biomarkers for geologists: a practical guide to the application of steranes and triterpanes in petroleum geology, American Association of Petroleum Geologists, Tulsa, Okla., U.S.A, 1991.
[37] A.P. Murray, C.J. Boreham, Organic geochemistry in petroleum exploration, Australian Geological Survey Organization, Canberra (1988) 230pp.
[38] K. Peters, C. Walters, J.M. Moldowan, The Biomarker Guide 2: Biomarkers and Isotopes in Petroleum Exploration and Earth History, 2d ed.: Cambridge, United Kingdom, Cambridge University Press, 2 (2005) 704 p.
[39] J.S. Sinninghe Damsté, T.I. Eglinton, J.W. De Leeuw, P.A. Schenck, Organic sulphur in macromolecular sedimentary organic matter: I. Structure and origin of sulphur-containing moieties in kerogen, asphaltenes and coal as revealed by flash pyrolysis, Geochimica et Cosmochimica Acta 53 (1989) 873–889. https://doi.org/10.1016/0016-7037(89)90032-X.
[40] A. Mostafa, E. Klitzsch, G. Matheis, H. Ganz, Origin and evaluation of hydrocarbons in the Gulf of Suez basin, Egypt, in: Geoscientific Research in Northeast Africa, in U. Thorweihe and H. Schandelmeier, eds.Geoscientific research in north east Africa, CRC Press, Rotterdam, Balkema, 1993: p. .267-275.
[41] Aquino Neto F.R., J.M. Trendel, A. Restle, Connan J., Albrecht P., Occurrence and formation of tricyclic and tetracyclic terpanes in sediments and petroleum., In: Bjorøy, M., Albrecht, C., Cornford, C., et al. (Eds.), Advances in Organic Geochemistry 1981. John Wiley and Sons,New York (1983) 659–676.
[42] G. Ourisson, P. Albrecht, M. Rohmer, Predictive microbial biochemistry — from molecular fossils to procaryotic membranes, Trends in Biochemical Sciences 7 (1982) 236–239. https://doi.org/10.1016/0968-0004(82)90028-7.
[43] J.M. Moldowan, W.K. Seifert, E.J. Gallegos, Relationship Between Petroleum Composition and Depositional Environment of Petroleum Source Rocks, Bulletin 69 (1985). https://doi.org/10.1306/AD462BC8-16F7-11D7-8645000102C1865D.
[44] E.A. Subroto, R. Alexander, R.I. Kagi, 30-Norhopanes: their occurrence in sediments and crude oils, Chemical Geology 93 (1991) 179–192. https://doi.org/10.1016/0009-2541(91)90071-X.
[45] J.S. Sinninghe Damsté, F. Kenig, M.P. Koopmans, J. Köster, S. Schouten, J.M. Hayes, J.W. de Leeuw, Evidence for gammacerane as an indicator of water column stratification, Geochimica et Cosmochimica Acta 59 (1995) 1895–1900. https://doi.org/10.1016/0016-7037(95)00073-9.
[46] J.E. Zumberge, Terpenoid biomarker distributions in low maturity crude oils, Organic Geochemistry 11 (1987) 479–496. https://doi.org/10.1016/0146-6380(87)90004-0.
[47] J.M. Moldowan, J. Dahl, B.J. Huizinga, F.J. Fago, L.J. Hickey, T.M. Peakman, D.W. Taylor, The Molecular Fossil Record of Oleanane and Its Relation to Angiosperms, Science 265 (1994) 768–771. https://doi.org/10.1126/science.265.5173.768.